

The Holocene

<http://hol.sagepub.com/>

Blue Intensity for dendroclimatology: The BC blues: A case study from British Columbia, Canada

Rob Wilson, Rohit Rao, Milos Rydval, Cheryl Wood, Lars-Åke Larsson and Brian H Luckman

The Holocene published online 12 August 2014

DOI: 10.1177/0959683614544051

The online version of this article can be found at:

<http://hol.sagepub.com/content/early/2014/08/12/0959683614544051>

Published by:



<http://www.sagepublications.com>

Additional services and information for *The Holocene* can be found at:

Email Alerts: <http://hol.sagepub.com/cgi/alerts>

Subscriptions: <http://hol.sagepub.com/subscriptions>

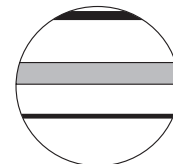
Reprints: <http://www.sagepub.com/journalsReprints.nav>

Permissions: <http://www.sagepub.com/journalsPermissions.nav>


Citations: <http://hol.sagepub.com/content/early/2014/08/12/0959683614544051.refs.html>

>> [OnlineFirst Version of Record](#) - Aug 12, 2014

[What is This?](#)



Blue Intensity for dendroclimatology: The BC blues: A case study from British Columbia, Canada

The Holocene
1–11
© The Author(s) 2014
Reprints and permissions:
sagepub.co.uk/journalsPermissions.nav
DOI: 10.1177/0959683614544051
hol.sagepub.com


Rob Wilson,¹ Rohit Rao,¹ Miloš Rydval,¹ Cheryl Wood,¹ Lars-Åke Larsson² and Brian H Luckman³

Abstract

Maximum latewood density (MXD) is a strong proxy of summer temperatures. Despite this, there is a paucity of long MXD chronologies in the Northern Hemisphere, which limits large-scale tree-ring-based reconstructions of past temperature which are dominated by ring-width (RW) data – a weaker temperature proxy at inter-annual time-scales. This paucity likely results from the relative expense of measuring MXD and the lack of laboratories with the facilities to measure it. Herein, we test the ability of a relatively new, less expensive, tree-ring parameter, Blue Intensity (BI), to act as a surrogate parameter for MXD. BI was measured on Engelmann spruce samples from British Columbia where MXD had previously been measured to allow direct comparison between the two parameters. Signal strength analyses indicate that 8 MXD series were needed to acquire a robust mean chronology while BI needed 14. Utilising different detrending methods and parameter choices (RW + MXD vs RW + BI), a suite of reconstruction variants was developed. The explained variance from the regression modelling (1901–1995) of May–August maximum temperatures ranged from 52% to 55%. Validation tests over the earlier 1870–1900 period could not statistically distinguish between the different variants, although spectral analysis identified more lower frequency information extant in the MXD-based reconstructions – although this result was sensitive to the detrending method used. Ultimately, despite the MXD-based reconstruction explaining slightly more of the climatic variance, statistically robust reconstructions of past summer temperatures were also derived using BI. These results suggest that there is great potential in utilising BI for dendroclimatology in place of MXD data. However, more experimentation is needed to understand (1) how well BI can capture centennial and lower frequency information and (2) what biases may result from wood discolouration, either from species showing a distinct heartwood/sapwood boundary or from partly decayed sub-fossil samples.

Keywords

Blue Intensity, British Columbia, Canada, dendroclimatology, Engelmann spruce, maximum density, maximum summer temperatures

Received 12 December 2013; revised manuscript accepted 22 June 2014

Introduction

Multiple tree-ring studies from the last few decades have clearly shown that maximum latewood density (MXD) chronologies, developed from conifer trees from high elevation/latitude environments, express a superior summer temperature signal than their ring-width (RW) counterparts (Büntgen et al., 2006; Esper et al., 2010, 2012; Grudd, 2008; Hughes et al., 1984; Luckman and Wilson, 2005; Schweingruber and Briffa, 1996; Wilson and Luckman, 2003). Although calibrated MXD chronologies have been shown to significantly diverge below summer temperatures for multiple sites around the Northern Hemisphere (Briffa et al., 2001), more recent studies, using updated data-sets and alternative detrending methods, have shown that MXD appears to track summer temperatures well (Anchukaitis et al., 2013; Esper et al., 2010; Wilson et al., 2007a) even in regions where RW expresses serious so-called ‘divergence’ (D’Arrigo et al., 2008). However, these observations need to be tested further at other sites. Despite the strength of MXD as a proxy of past summer temperatures, few millennial length MXD records exist (Büntgen et al., 2006; Esper et al., 2012; Grudd, 2008; Luckman and Wilson, 2005), and therefore, tree-ring-based large-scale composites of Northern Hemispheric temperatures are derived mostly from RW data (D’Arrigo et al., 2006; Frank et al., 2007).

The paucity of millennial length MXD chronologies contrasts with the many long temperature sensitive RW chronologies that are available (Biondi et al., 1999; Cook et al., 2013; D’Arrigo et al., 2001; Esper et al., 2003; Hughes et al., 1999; Salzer and Kipfmüller, 2005; Wilson et al., 2007b). Ultimately, this situation simply comes down to cost and the fact that few institutions have the facilities to measure density parameters. This is an unusual situation, given the importance placed upon tree-ring data for understanding late Holocene temperature variability (Jones et al., 2009).

The situation recently came to a head when Mann et al. (2012) hypothesised that there was a high probability that tree-ring chronologies underestimated volcanically forced cooler temperatures because of the fact that for some severe volcanic events (e.g.

¹University of St Andrews, UK

²Cybis Elektronik & Data AB, Sweden

³University of Western Ontario, Canada

Corresponding author:

Rob Wilson, University of St Andrews, North Street, St Andrews, KY16 9AL, UK.

Email: rjsw@st-andrews.ac.uk

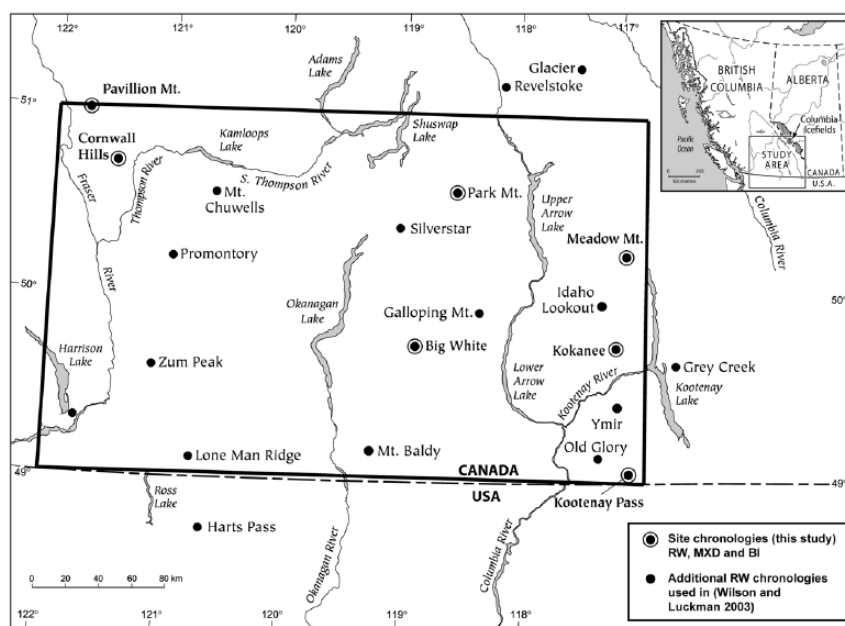


Figure 1. Location of study region. The 21 tree-ring sites used in Wilson and Luckman (2003) are shown. Herein, we utilise only the 7 sites where ring-width (RW), maximum latewood density (MXD) and blue intensity (BI) were measured. The box denotes the CRUTS3.1 gridded data-set (Harris et al. (2014) – 122–117°W/49–51°N) used for growth-climate analyses and calibration/verification.

1258, 1453 and 1815), trees failed to put on growth rings over large regions. Anchukaitis et al. (2012) rebutted this hypothesis by highlighting the simple fact that the D'Arrigo et al. (2006) Northern Hemispheric reconstruction (used in Mann et al., 2012) utilised almost entirely RW data which poorly track inter-annual variability, and their RW-based reconstruction was therefore a poor proxy composite series to study volcanic forcing (see also D'Arrigo et al., 2013; Esper et al., 2013a, 2013b). This paper is not the place to re-iterate the arguments of Mann et al. (2012) and Anchukaitis et al. (2012). However, this contentious issue did highlight that for robust attribution of climate forcing of the last 1000 years – especially with respect to the influence of volcanic events – more MXD chronologies need to be developed, especially prior to 1500. As MXD data appear problematic for most laboratories to generate, this paper emphasises the potential of a relatively new tree-ring parameter – Blue Intensity (BI) – which could be used as an alternative to MXD to overcome this issue.

Assuming that most tree-ring laboratories initially create RW chronologies, but ultimately struggle to acquire funds to measure MXD, a less expensive alternative to MXD would be desirable. MXD is a measure of latewood density, which reflects lignin content in the latewood (Gindl et al., 2000). Lignin is controlled by summer temperatures – that is, a warm summer leads to increased lignin content which results in a denser/darker latewood. Early studies suggested that reflected light from scanned images of wood could provide a reasonable proxy similar to wood density (Sheppard et al., 1996; Yanosky and Robinove, 1986). These initial experimentations were further refined by McCarroll et al. (2002) who showed that lignin absorbed more light in the visible blue domain of the light spectrum and that latewood minimum blue reflectance (hereafter referred to as BI) could provide a substantially cheaper proxy portraying similar information to MXD. Campbell et al. (2007, 2011), Babst et al. (2009), Wilson et al. (2011), Björklund et al. (2014) and Rydval et al. (2014) have continued experimentation with BI highlighting the significant potential of this parameter as an alternative measure of the cost-intensive lignin measurements based on radiodensitometric techniques. However, despite all of this promising experimental work, no specific BI-based temperature reconstruction has been published to date.

Herein, we use tree samples from British Columbia (BC), Canada, from which Wilson and Luckman (2003) developed RW and MXD data to derive a summer maximum temperature reconstruction for the region back to 1600. The original network consisted of 21 Engelmann spruce RW chronologies plus 7 MXD chronologies developed for the longest records. Using the same samples that were used to derive MXD in the original study, we have measured BI using CooRecorder (Larsson, 2013; see also detailed methods in Rydval et al. (2014)) to derive, for the first time, BI measurements that can be directly compared to traditionally radiodensitometric derived MXD data for a network of sites. The replication of the Wilson and Luckman (2003) study using BI is a particularly good test for this new parameter as (1) Engelmann spruce shows no visible colour change between heartwood and sapwood which can potentially bias any reflectance based measures (Björklund et al., 2014; Rydval et al., in preparation; Sheppard and Wiedenhoef, 2007) and (2) the original reconstruction was strongly calibrated ($r^2=53\%$) and later verified using an independent reconstruction from a neighbouring region (Luckman and Wilson, 2005). This study therefore provides an optimal scenario for testing BI as an alternative, cheaper, proxy archive to MXD for reconstructing past summer temperatures.

Data and methods

Chronology development

We focus on the seven sites from Wilson and Luckman (2003) from which MXD was measured (Figure 1). Data from the other 14 sites were not used. In the original study, density was measured using radiodensitometric techniques (Schweingruber et al., 1978) from 0.3-mm-thick microtomed sections along each core. In this study, the BI data were measured on the remaining core from which the microtomes were originally taken. As spruce does not express an obvious visible colour difference between the heartwood and sapwood, no pre-treatment (i.e. resin extraction) of the samples was made and the mounted cores were simply sanded up to 1200 grit grade. Residual wood dust was removed using compressed air. We followed the procedures

detailed in Rydval et al. (in preparation) to generate the BI data. The scanner was calibrated using the SilverFast Auto IT8 Calibration procedure to the IT8 Calibration Target (IT8.7/2) printed on Kodak Professional Endura paper. All samples were scanned to 2400 DPI with the scanner covered by a box to minimise bias from external ambient light. The digital image of each sample was then imported into CooRecorder and the ring-boundaries marked and visually crossdated. BI data were then generated using frame dimensions (160-5-50-15) derived from experimentation with Scots pine (Rydval et al., 2014). As BI is inversely correlated with MXD (i.e. a dense dark latewood will express low reflectance), and to ensure consistency for the proxy comparison, the raw BI data were inverted to allow the same detrending procedures to be used for both data types. To do this, all BI values were multiplied by -1 and a constant of 2.56 (related to the standard light intensity scale of 0 to 255) added to ensure all inverted values were positive. No other transformation of the raw BI data was performed.

Our main aim is to replicate, as best as possible, the Wilson and Luckman (2003) study using BI data instead of MXD. Therefore, detrending was initially performed in the same manner as the original study. The RW data, from the same seven sites, were individually detrended via division using negative exponential or linear (negative or zero slope) functions. The MXD and BI data were detrended via subtraction of linear (negative or zero slope) functions only. We are aware that these approaches are perhaps no longer 'state of the art' with respect to detrending. However, it is important to follow the original methodology as closely as possible for comparison with the original Wilson and Luckman (2003) results. For this study, we will call these chronology versions 'Standard' (STD). We also experiment, however, with the later developed 'Signal-Free' (SF) detrending approach (Melvin and Briffa, 2008) which should produce chronologies less biased in the mid-lower frequencies. We do not experiment with the Regional Curve Standardisation approach (Briffa and Melvin, 2010) as it is not a suitable approach for detrending data from living trees alone. However, it should be emphasised that the potential removal of lower frequency information is not so significant in a situation where warming occurs from the 'Little Ice Age' (LIA) to present (see Luckman and Wilson, 2005) because we are essentially only removing age-related negative trends in the raw tree-ring series. This detrending bias would be much more relevant for the transition from the warm medieval to 'LIA'. For all chronologies, the variance was temporally stabilised using techniques outlined in Osborn et al. (1997).

The mean between-series correlation (RBAR) and Expressed Population Statistic (EPS – Briffa and Jones, 1990) were used to assess the signal strength of the parameter detrended series as well as to assess how many series are needed to acquire a robust mean function that represents the 'true' infinitely replicated population chronology (see Wilson and Elling, 2004). Principal component analysis (using a varimax rotation) was performed over the period where the EPS was ≥ 0.85 (Wigley et al., 1984) for all the parameter chronologies to assess the between parameter coherence. A further rotated PCA was performed on the seven chronologies of each parameter to derive an optimal time-series of common variance for each parameter. This parameter-specific PC score was then compared to a parameter-specific mean composite where all the data from the seven sites for each parameter were pooled together to derive a longer parameter-specific regional chronology. The EPS is again used to quantify the decrease in signal strength back in time as replication decreases. The PC scores are limited in temporal extent because of the EPS 0.85 threshold used. However, as done in Wilson and Luckman (2003), the pooled regional mean composites allowed the extension of any potential reconstruction back prior to the common period used for the PCA.

Correlation response function analysis and dendroclimatic reconstruction

As in Wilson and Luckman (2003), we used both mean (hereafter Tmean) and maximum (hereafter Tmax) temperatures from the CRUTS3.1 gridded data-set (Harris et al. (2014) – 122–117°W/49–51°N – Figure 1). Correlations were calculated (hereafter referred to as correlation response function analysis (CRFA)) between the parameter-specific regional composites and monthly variables of temperature from previous April through to current September over the 1901–1995 period.

The regional mean composite chronologies were used to derive extended reconstructions back prior to the period covered by the PCA. Both STD and SF chronology versions were used to derive different variants of past temperatures, and all chronologies were lagged at T and T+1, for the multiple regression, to allow the potential modelling of the previous year's climate influence on growth (as done by Wilson and Luckman, 2003). The target season for reconstruction was chosen based on the CRFA results and calibration experiments against a number of different summer seasons. Full period calibration was undertaken over the 1901–1995 period, while split period calibration and verification were performed on the 1901–1947/1948–1995 periods, respectively. For verification, we utilised the Coefficient of Efficiency (CE – Cook et al., 1994) and tested the residuals from the full period calibration for autocorrelation (using the Durbin–Watson (DW) statistic) and linear trends. A robust regression model should result in residual values with no autocorrelation and no linear trends.

As a suite of different reconstructions were developed using RW/MXD and RW/BI combinations as well as both STD and SF detrending, an additional test of the reconstructions was employed to ascertain which of the different versions could be deemed most robust. We extracted relevant climate data from the Berkeley Earth Surface Temperature (BEST – Rohde et al., 2013) data-set for a 1° larger grid (123–116°W/48–52°N) than used for calibration with the CRUTS3.1 data. The resultant temperature series extends back to 1870. The different reconstruction variants, including the Wilson and Luckman (2003) Interior British Columbia (IBC) reconstruction, were scaled (Esper et al., 2005) to the BEST data over the 1901–1995 period, and the root mean square error (RMSE) calculated for the 1870–1900 period. Hypothetically, assuming no significant homogeneity issues in the instrumental data (Peterson et al., 1998), the least biased reconstruction with respect to its ability to capture mid-to-low frequency variability should better match the instrumental data outside the 1901–1995 calibration period resulting in a lower RMSE value. To further assess the performance of the different reconstruction variants to capture lower frequency variability, coherency spectral analysis was performed over the 1901–1995 (CRUTS3.1) and 1870–1995 (BEST) periods and spectral density functions calculated over the full period of the reconstructions (1600–1995).

Results and discussion

Chronology properties

Table 1 presents basic chronology and signal strength statistics for each site and parameter. By calculating the coefficient of variation (CV) between the individual raw series for each parameter and site, the RW data expresses greatest relative between-series variance when assessing all seven sites (mean CV=0.28). This is not surprising as growth rates between trees and sites can be quite varied because of tree and site specific ecological differences. MXD, on the other hand, more strongly controlled by summer temperatures (Wilson and Luckman, 2003), is known to be much less influenced by site specific factors which are clearly supported by the lower mean CV value of 0.19. MXD also expresses

Table 1. Basic summary statistics for each site and parameter.

	No. of series (trees)	Ring-width (RW)					Maximum latewood density (MXD)					Blue Intensity (BI)				
		MEAN	STDEV	CV	RBAR	<i>n</i> for EPS (0.85)	MEAN	STDEV	CV	RBAR	<i>n</i> for EPS (0.85)	MEAN	STDEV	CV	RBAR	<i>n</i> for EPS (0.85)
Meadow Mt	38 (23)	0.84	0.25	0.30	0.29	14	0.89	0.14	0.16	0.49	6	1.11	0.04	0.04	0.31	12
Kokanee	30 (19)	1.23	0.33	0.27	0.24	18	0.84	0.14	0.16	0.36	10	1.00	0.04	0.04	0.29	14
Kootenay	56 (19)	1.26	0.27	0.21	0.27	15	1.05	0.21	0.20	0.41	8	1.07	0.07	0.07	0.31	13
Park Mt	38 (25)	0.86	0.33	0.38	0.33	11	0.72	0.17	0.23	0.39	9	1.08	0.07	0.06	0.27	16
Big White	35 (27)	0.91	0.23	0.25	0.22	20	0.78	0.18	0.23	0.36	10	0.98	0.07	0.07	0.27	15
Pavilion	35 (23)	1.17	0.31	0.27	0.42	8	0.75	0.13	0.17	0.50	6	1.05	0.04	0.04	0.32	12
Cornwall Hills	35 (22)	0.95	0.28	0.29	0.35	11	0.87	0.18	0.21	0.45	7	1.13	0.05	0.04	0.30	13
MEAN	38 (23)	1.03	0.29	0.28	0.30	14	0.84	0.16	0.19	0.42	8	1.06	0.06	0.05	0.30	14

No. of series: no individual measured series and trees in parentheses; MEAN: mean measurement for each site chronology; STDEV: standard deviation between mean values of all series in the parameter chronology; CV: coefficient of variation (standardised measure of variation (MEAN/STDEV)); RBAR: mean inter-series correlation of all possible bivariate combinations between the detrended series. RW = mms; MXD = g/cm³; BI = reflectance intensity $\times 10^2$. Note that BI values were not inverted for these calculations; *n* for Expressed Population Statistic (EPS) (0.85) = the number of series needed to acquire an EPS value of 0.85 – see Wilson and Elling (2004) for method.

a stronger common signal with a mean inter-series correlation (RBAR) of 0.42 as opposed to 0.30 for RW. The range in mean BI values, however, is more constrained than MXD with an overall CV of 0.05 which suggests that this parameter is quite insensitive to between site differences. At this stage, it is not clear whether this is a positive or negative aspect of this parameter. The mean RBAR for the BI data is 0.30, the same as RW, which identifies MXD as the parameter with the strongest common signal – therefore requiring fewer trees series (8 vs 14) to derive a robust chronology mean.

A rotated varimax PCA using all 21 parameter chronologies was undertaken over the 1811–1996 period where EPS was greater than 0.85 in all chronologies. Figure 2 presents the loadings of each parameter chronology on the first two eigenvectors as well as a bivariate scatter plot of these loadings. PC1 explains 53.8% of the overall variance and is dominated by both the MXD and BI chronologies which cluster together in the bivariate plot. However, although these results indicate that the BI data express a similar signal to MXD, the loadings of the BI chronologies are on average marginally weaker on PC1 than their MXD counterparts. This supports the observation that the common signal in the BI chronologies is weaker than MXD (Table 1). PC2, explaining 21.6% of the variance, is dominated by the RW chronologies.

PCA (1811–1996) was rerun on the seven chronologies for each parameter, and regional parameter composite chronologies were derived by pooling all the data from each site. For each parameter, one eigenvector was identified as significant with MXD showing the strongest parameter-specific between chronology common signal (explained variance = 85.1%), followed by BI (76.1%) and finally RW (67.3%). Figure 3 compares the parameter-specific PC scores with their regional mean composite counterparts (normalised to z-scores relative to the 1811–1996 period). For each parameter, the correlation between the PC score and the regional composite is very strong ($r > 0.99$), indicating that using the regional parameter composite chronologies would be an appropriate method to derive as long a reconstruction as possible from these data. However, the signal quality of these parameter regional composites will decrease back in time as replication decreases. EPS, calculated for running 30-year windows, shows that signal strength starts weakening for all parameters in the 17th century. For MXD, EPS falls below 0.85 around the 1620s, but for BI, which has a weaker common signal (Table 1), EPS starts dropping below this threshold value around 1700 and plummets to zero in the early 17th century. The RW

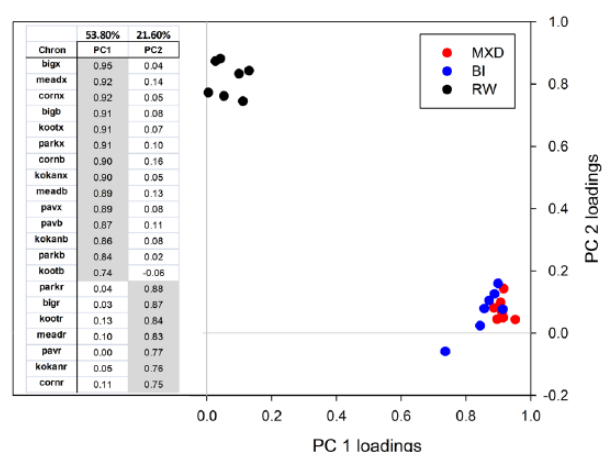


Figure 2. Scatter plot of Principal Component Analysis loadings of each chronology on the first two eigenvectors. After the chronology ID, x denotes MXD, b denotes BI and r denotes RW. MXD: maximum latewood density; BI: Blue Intensity; RW: ring-width.

composite drops below the 0.85 threshold around the 1640s. All analyses hereafter utilise the longer regional parameter composite chronologies as they express the same signal as the parameter PC scores over the well replicated 1811–1996 period and provide information back to 1600.

Correlations between the parameter composite chronologies over the 1811–1996 and 1600–1810 periods (Table 2) show that MXD and BI are strongly correlated ($c \geq 0.9$). Coherence of the MXD and BI chronologies with RW is weak at best and is only significant for the 1811–1996 period and marginally higher (0.31 and 0.37) when the series are first differenced. Overall, the PCA (Figure 2) and between parameter correlations indicate that the BI data appear to express a very similar signal to MXD, while RW portrays essentially unique variance.

CRFA and dendroclimatic reconstruction

Wilson and Luckman (2003) noted that optimal calibration using the BC tree-ring data was against maximum summer temperatures rather than the more traditional mean temperatures used in most dendroclimatic studies. They hypothesised that this was logical as most of the tree's cambial activity, with respect to

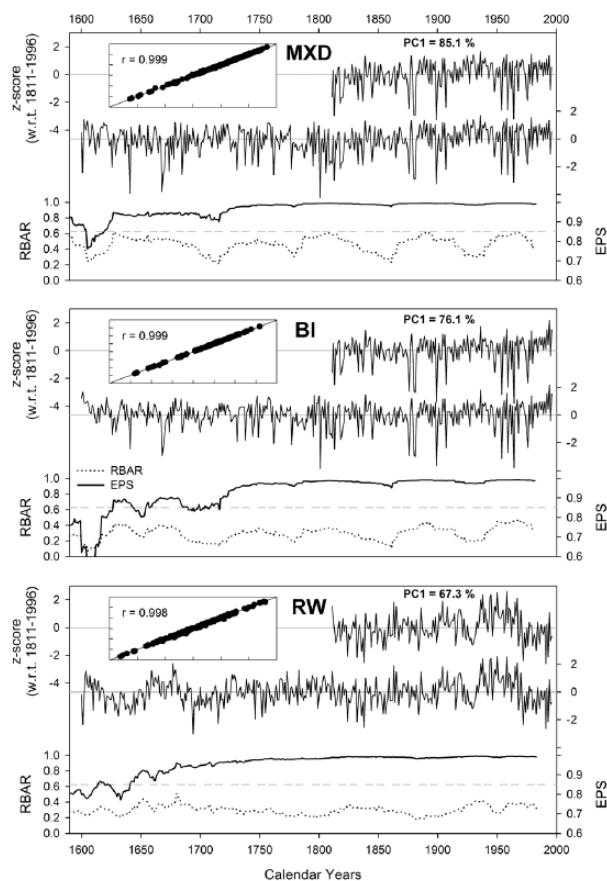


Figure 3. Time-series plots of the parameter PC scores (1811–1996), regional composites (1600–1996) and running 30-year RBAR and EPS series. The PCA was run separately for each of the 7 parameter chronologies. The explained variance on the first and only eigenvector is shown for each parameter. The scatter plot indicates the strong linear relationship between the PC score and the regional composites. MXD: maximum latewood density; BI: Blue Intensity; RW: ring-width; EPS: Expressed Population Statistic.

Table 2. Between parameter correlations using the STD detrended regional composite chronologies. Analysis was performed over the 1600–1810 and 1811–1996 periods. Greyed values are for first differenced transforms.

1811–1996				1600–1810			
	MXD	BI	RW		MXD	BI	RW
MXD		0.96**	0.16*	MXD		0.89**	0.05
BI	0.99**		0.17*	BI	0.91**		0.08
RW	0.31**	0.37**		RW	0.10	0.10	

MXD: maximum latewood density; BI: Blue Intensity; RW: ring-width.
*Correlations significant at the 95% confident limits; **correlations significant at the 99% confident limits.

photosynthesis, occurs during the day. This hypothesis has not yet been specifically rejected and has been shown to hold in the Yukon (Youngblut and Luckman, 2008) and the Pyrenees (Büntgen et al., 2008). We return again to this hypothesis to see whether it holds for the BI parameter as well. Figure 4 presents the CRFA results between the parameter regional chronologies and monthly/seasonal variables of mean (Tmean) and maximum (Tmax) temperatures. Despite the weaker common signal noted for the BI data (Table 1), the response of MXD and BI is very similar with

both parameters showing a broad response to current year temperatures from March to August, but with August showing substantially stronger (>0.65) correlations. Strongest correlations are noted for Tmax. MXD correlations with MJJA (August) Tmax are 0.67 (0.72), as opposed to 0.66 (0.70) for BI. The first differenced correlations for the same season (month) are 0.71 (0.77) for MXD and 0.72 (0.76) for BI. As shown by Wilson and Luckman (2003), correlations are weaker for RW but are still stronger for Tmax than Tmean. RW appears to be controlled by a slightly earlier seasonal window and correlates most strongly with June–July Tmax. There is, however, a notable improvement in correlations when the data are first differenced, from 0.44 (non-transformed correlation) to 0.68, suggesting that the response of RW data is stronger at inter-annual time-scales and weaker at mid-longer time-scales. Despite these observations, we can state that June–July temperatures are the dominant control of year-to-year RW variability. All parameters portray inverse correlations with previous year's summer temperatures – specifically August for MXD and BI, and July–August for RW – hence the utilisation of lagged (T and T+1) variables in the regression modelling.

Utilising STD and SF chronology versions for RW, MXD and BI, a range of experimental trial calibrations (1901–1995) were made for different summer seasons of Tmean and Tmax (Table 3). The explained variance (a^2) was generally high, ranging from c. 0.3 to 0.6. As well as the a^2 values, the residuals from the regression modelling were tested for autocorrelation (using the DW) and linear trends to provide other metrics to ascertain which seasonal target would be optimal for reconstruction. Except for August, all calibrations with Tmean resulted in model residuals that either expressed significant autocorrelation or linear trends or both. For Tmax, best calibration results were obtained for August, JJA and MJJA. Although the highest a^2 values were obtained for the JJA season, it was felt that MJJA should be utilised for reconstruction as the residuals from the JJA modelling expressed slight residual autocorrelation (DW < 1.5) when using the BI data and that the MJJA season would be consistent with the results of Wilson and Luckman (2003) who also reconstructed Tmax MJJA temperatures. The IBC reconstruction of Wilson and Luckman (2003) explained 53% of the temperature variance. The new results are comparable with the STD (SF) versions for both the RW-MXD and RW-BI combinations explaining 54% (55%) and 52% (53%) of the temperature variance, respectively.

Figure 5a presents the split period calibration and verification results for each of the RW-MXD and RW-BI combinations. In general, the RW-MXD based reconstructions calibrate slightly more strongly than the RW-BI versions, while the SF detrended chronologies are marginally better than STD. However, the differences are slight. Verification using the CE is also equally robust for all variants. The most stable calibration and verification results over the two periods are with the RW-BIstd variant. Coherency spectral analysis of the four reconstruction variants with Tmax MJJA (Figure 5b), however, suggests that the BI-based reconstructions struggle to capture temperature variability at time-scales longer than ~20 years. This is an important observation as, ideally, a tree-ring-based reconstruction should capture variability at all time-scales. If the BI parameter is somehow systemically limited with respect to its ability to capture longer time-scale information, this requires further examination.

Figure 6a presents the four reconstruction variants along with the IBC (Wilson and Luckman, 2003) and Icefields (ICE – Luckman and Wilson, 2005) reconstructions. All series are calibrated to the same Tmax MJJA season. Visually, it is clear that there is a marked amplitude difference between the different reconstruction variants with the RW-BIstd (low) and RW-MXDsf (high) being the most extreme end members. Table 4 presents the amplitude difference between the reconstructions for the coldest (1777–1826) and warmest (1922–1971) 50-year

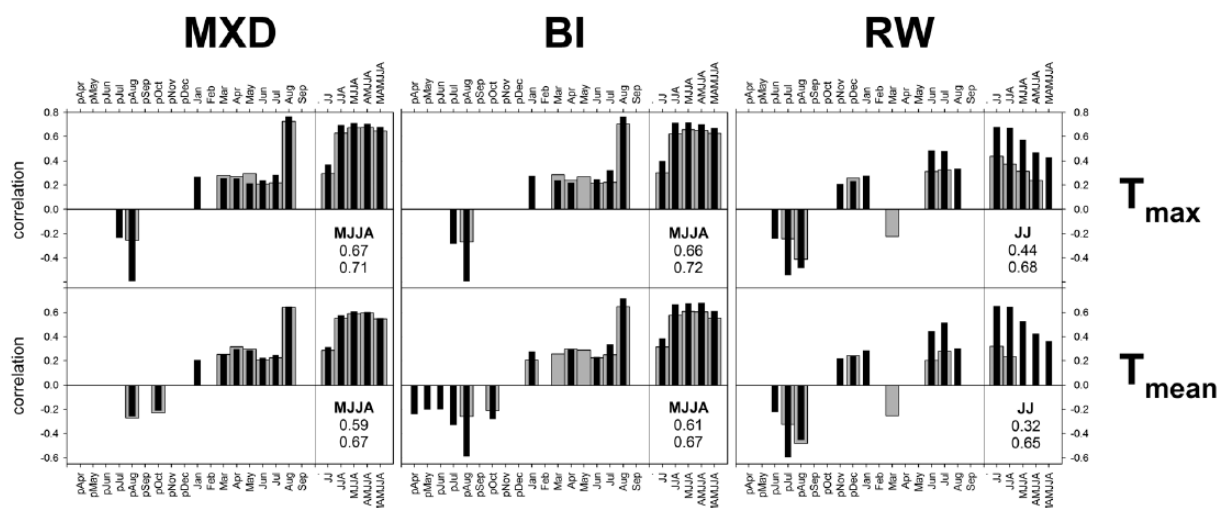


Figure 4. Correlation response function analysis results (1901–1995). Significant (95% confidence limit (CL)) correlations are shown between each parameter regional composite chronology and monthly and seasonal variables of maximum and mean CRUTS3.1 temperatures. Grey bars are correlations using non-transformed series while black bars are correlations after the time-series have been transformed to first differences. MXD: maximum latewood density; BI: Blue Intensity; RW: ring-width.

Table 3. Calibration (1901–1995) trials for a variety of Tmean (*m*) and Tmax (*x*) seasonal parameters.

STD recon: RW and MXD					SF recon: RW and MXD				
	a_r^2	Variables	DW	Lin r		a_r^2	Variables	DW	Lin r
Augm	0.49	MXD, bRW, bMXD	2.03	0.26	Augm	0.50	MXD, bRW	2.15	0.12
JJAm	0.48	MXD, bRW, RW	1.41	0.39	JJAm	0.52	MXD, bRW, RW	1.51	0.31
MJJAm	0.40	MXD, bRW, RW	1.33	0.44	MJJAm	0.43	MXD	1.77	0.26
AMJJAm	0.36	MXD	1.42	0.42	AMJJAm	0.43	MXD	1.61	0.25
MAMJJAm	0.33	MXD, bRW	1.23	0.39	MAMJJAm	0.38	MXD	1.50	0.29
Augx	0.54	MXD, bRW	1.97	-0.03	Augx	0.52	MXD, bMXD	1.90	-0.13
JJAx	0.60	MXD, RW, bRW	1.55	0.05	JJAx	0.59	MXD, RW, bRW	1.53	-0.10
MJJAx	0.54	MXD, RW, bRW	1.64	0.15	MJJAx	0.55	MXD, RW, bRW	1.67	-0.04
AMJJAx	0.48	MXD, RW	1.86	0.14	AMJJAx	0.50	MXD, RW	1.87	-0.07
MAMJJAx	0.42	MXD	1.70	0.18	MAMJJAx	0.44	MXD	1.75	0.00
STD recon: RW and BI					SF recon: RW and BI				
	a_r^2	Variables	DW	Lin r		a_r^2	Variables	DW	Lin r
Augm	0.47	BI, bRW	2.07	0.20	Augm	0.48	BI, bRW	2.10	0.16
JJAm	0.49	BI, bRW, RW	1.42	0.36	JJAm	0.50	BI, bRW, RW	1.46	0.33
MJJAm	0.40	BI, bRW	1.44	0.35	MJJAm	0.42	BI	1.69	0.28
AMJJAm	0.37	BI	1.48	0.35	AMJJAm	0.41	BI	1.56	0.27
MAMJJAm	0.34	BI, bRW	1.30	0.36	MAMJJAm	0.35	BI	1.45	0.31
Augx	0.51	BI, bBI	1.88	-0.02	Augx	0.50	BI, bBI	1.87	-0.09
JJAx	0.58	BI, RW, bRW	1.49	0.00	JJAx	0.57	BI, RW, bRW	1.49	-0.07
MJJAx	0.52	BI, RW, bRW	1.63	0.08	MJJAx	0.53	BI, RW, bRW	1.64	0.00
AMJJAx	0.46	BI, RW	1.80	0.05	AMJJAx	0.47	BI, RW	1.80	-0.04
MAMJJAx	0.41	BI	1.68	0.11	MAMJJAx	0.42	BI	1.69	0.02

RW: ring-width; MXD: maximum latewood density; DW: Durbin–Watson statistic for residual autocorrelation; BI: Blue Intensity; Lin R: correlation between residuals and time.

The variables column denotes which chronology versions entered the multiple regression model; b denotes a chronology lagged at $T + 1$; grey values denote significant autocorrelation and/or significant residual linear trend or both.

periods. As expected, RW-BIstd expresses the smallest temperature difference of only 0.27°C , while RW-MXDsf shows a much larger change of 1.30°C . Utilising the CRUTS3.1 data, it is not possible to ascertain which of these two variants is most robust, although the coherency analysis (Figure 5b) suggests

that the RW-MXDsf reconstruction may capture longer time-scale information more robustly. The spectral density functions of the six reconstructions (Figure 6b) clearly show that the greatest difference between the series is at time-scales > 50 years. RW-MXDsf shows the greatest spectral

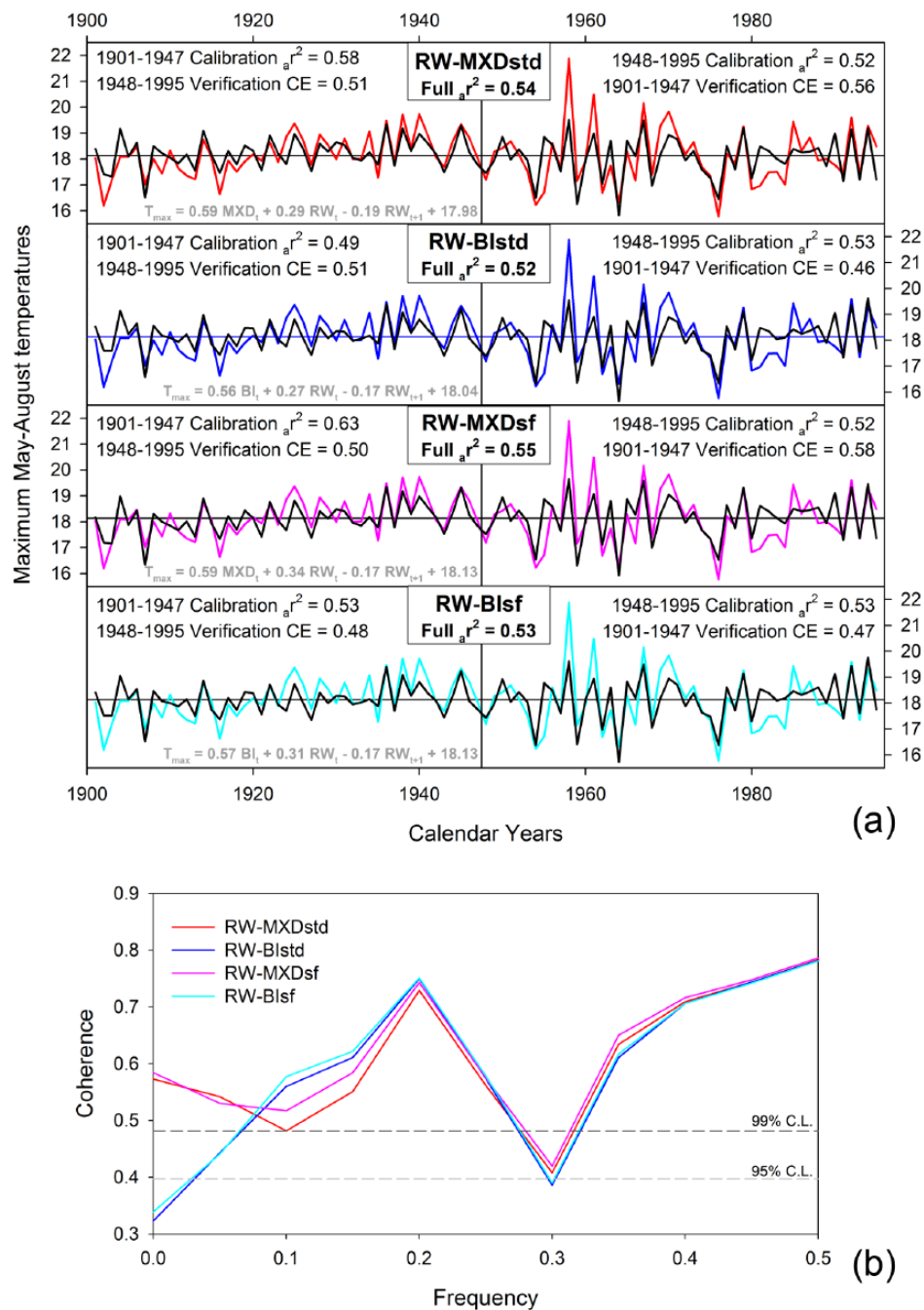


Figure 5. (a) Full and split period calibration/verification results for the four chronology/parameter variants for British Columbia. Full period regression equations are shown in grey. (b) Coherency spectra between the reconstructions and MJJA T_{max} temperatures. RW: ring-width; MXD: maximum latewood density; BI: Blue Intensity.

power at centennial and longer time-scales, while RW-Blst shows the least.

The only way to ascertain potentially which of the reconstructions better portrays longer time-scale information is to compare the series to independent temperature data prior to the 1901–1995 calibration period. This early period is important as it encompasses the late phase of the LIA where the different reconstruction variants start diverging (Figure 6a). The BEST (Rohde et al., 2013) data-set allowed this extended analysis. Each reconstruction from BC was scaled (Esper et al., 2005) over the 1901–1995 period to T_{max} MJJA using a 1° larger gridded region of the BEST data than that used for the CRUTS3.1 data. The correlation between the CRUTS3.1 and BEST data-sets is 0.98 which indicates that using this larger BEST grid identifies an appropriate pre-calibration data-set for comparison. The correlations and RMSE were calculated over the 1870–1900 period with the basic

hypothesis that those reconstruction variants that best track the early instrumental data should correlate most strongly with the temperature data and will also express lower RMSE values. Strongest correlations were found for RW-MXDstd and RW-MXDsf, while the lowest RMSE was found with RW-MXDstd (Table 5). However, the correlation and RMSE values for the BI variants are very similar.

These results highlight a frustrating reality for palaeoclimatology. For robust attribution of the drivers of climate change, we need to ensure that palaeoclimate reconstructions are applicable at all time-scales. This is, however, difficult to quantify with the relatively short instrumental record found in most regions of the world. In this case study, it is not possible to state specifically which reconstruction variant is the more robust. All of the variants pass traditional calibration and verification metrics (Figure 5) with an a^2 range from 0.52 to 0.55 for the 1901–1995 period.

When compared to earlier instrumental data, although the RW-MXDstd version expresses the ‘best fit’, the range in RMSE is 0.65–0.74, which equates to a 0.18°C 2-sigma error difference only. Therefore, we must view these five BC reconstruction variants as an ensemble of estimates of past MJJA maximum

temperatures which provide a likely realistic range for the past four centuries.

Using the RMSE values (Table 5), we developed a weighted mean of the five BC MJJA Tmax reconstructions so that the RW-MXDstd series, with the lowest RMSE, was weighted most strongly and the RW-MXDsf, with the highest RMSE, weighted least. This regional weighted series is hereafter referred to as the BC COMBO. Figure 7a presents coherency spectra of each of the individual five BC reconstructions and the BC COMBO series against the BEST MJJA Tmax data over the full 1870–1995 period. The IBC (Wilson and Luckman, 2003) series clearly shows weakest overall coherence, while the RW-MXDsf and BC COMBO series show greatest coherence – even at lower frequencies. We should note, however, that the RW-BIsf series also expresses good overall coherence, and if we only had RW and BI data, these results suggest a valid reconstruction could be derived without the use of MXD. The BC COMBO reconstruction with associated 2-sigma error bars is shown in Figure 7b (non-smoothed) and c (smoothed). The error bars are calculated using the RMSE estimates derived from the 1870–1900 period (Table 5) for both the non-smoothed and smoothed series and reflect the full combined 2-sigma error range expressed by all five reconstruction variants. The ICE reconstruction (Luckman and Wilson, 2005), where the MXD data had been processed using RCS, is also shown in Figure 7c. Despite a cooler deviation of the ICE series from *c.* 1670 to 1770, which likely reflects local extreme cooling influences on tree-growth because of the proximity of the Athabasca Glacier during that time, both reconstructions agree very well. Therefore, by combining the information from the five BC reconstruction variants, we believe that the BC COMBO series is a significant improvement on the original IBC reconstruction (Wilson and Luckman, 2003) with regards to understanding past summer temperature change in IBC for the last four centuries.

Summary and conclusion

The aim of this study was to test the validity of the relatively new tree-ring parameter, BI, as a surrogate for MXD to reconstruct past summer temperatures. To do this, we processed samples from which MXD had previously been measured (Wilson and Luckman, 2003) so that a direct comparison of the two parameters could be made. Signal strength statistics (Table 1) indicate that the between-series common signal for BI is weaker than MXD. While only 8 series are needed to derive a robust mean chronology using MXD, 14 series are needed for BI. However, this does not pose a significant problem because of the relative cheapness and quicker processing time for the development of BI data as more tree-ring samples can be measured. CRFA (Figure 4) indicates that the response of MXD and BI to monthly variables of summer temperature is very similar. However, marked differences in regression based reconstructed amplitudes were noted (Table 4) when using STD or SF approaches to detrending, although from calibration alone, little difference was noted between the different reconstruction variants (Figure 5 – a^2 range=52–55%). Even

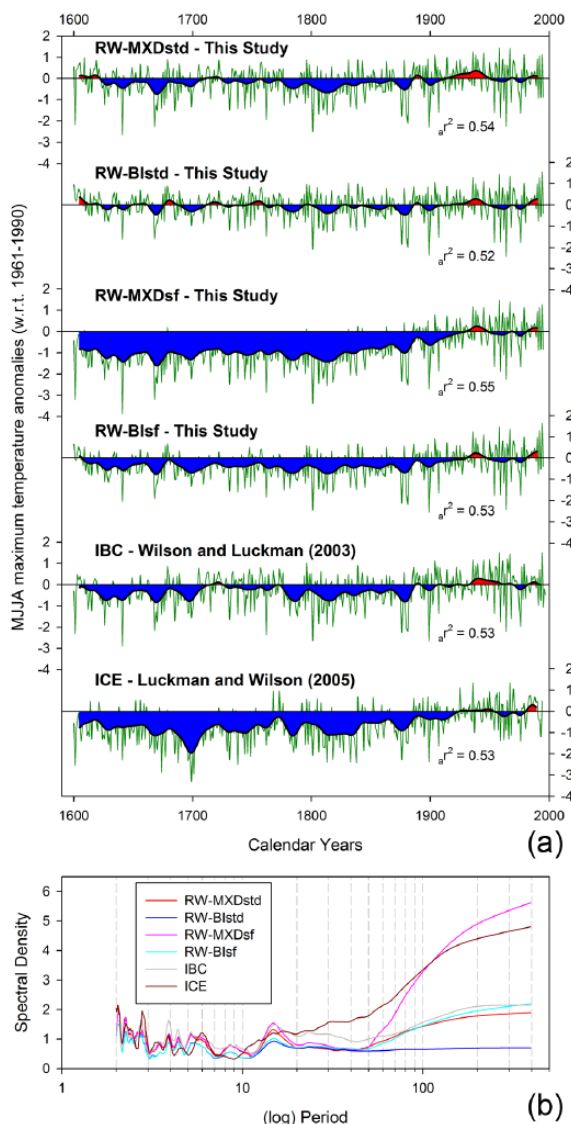


Figure 6. (a) Time-series plots (also smoothed with a 20-year smoothing spline (Cook and Peters, 1981)) of the four new reconstruction variants, plus the original Wilson and Luckman (2003) IBC reconstruction and neighbouring Canadian Rockies Icefields (ICE) reconstruction. All series are expressed as temperature anomalies (w.r.t. 1961–1990) and the explained variance for the full calibration is shown. (b) Spectral density analysis plot for each of the six reconstructions. RW: ring-width; MXD: maximum latewood density; BI: Blue Intensity; IBC: Interior British Columbia; ICE: Icefields.

Table 4. Temperature anomaly estimates for the coldest (1777–1826) and warmest (1922–1971) 50-year periods for the six MJJA Tmax reconstructions. These periods were identified by first averaging the six anomaly series together and then identifying the coldest/warmest 50-year period from this mean series.

	RW-MXDstd	RW-BIstd	RW-MXDsf	RW-BIsf	IBC	ICE
1777–1826	−0.47	−0.22	−1.26	−0.58	−0.57	−0.90
1922–1971	0.13	0.06	0.03	0.01	0.12	−0.01
Amplitude	0.60	0.27	1.30	0.59	0.70	0.89

RW: ring-width; MXD: maximum latewood density; BI: Blue Intensity; IBC: Interior British Columbia; ICE: Icefields.

Table 5. Correlation (r) and RMSE ($^{\circ}\text{C}$) calculated between the five BC reconstructions and the BEST MJJA Tmax data over the 1870–1900 period.

	RW-MXDstd	RW-BIstd	RW-MXDsf	RW-BIsf	IBC
r	0.77	0.73	0.77	0.74	0.75
RMSE	0.65	0.69	0.74	0.69	0.71

BEST: Berkeley Earth Surface Temperature; RW: ring-width; MXD: maximum latewood density; BI: Blue Intensity; IBC: Interior British Columbia; RMSE: root mean square error.

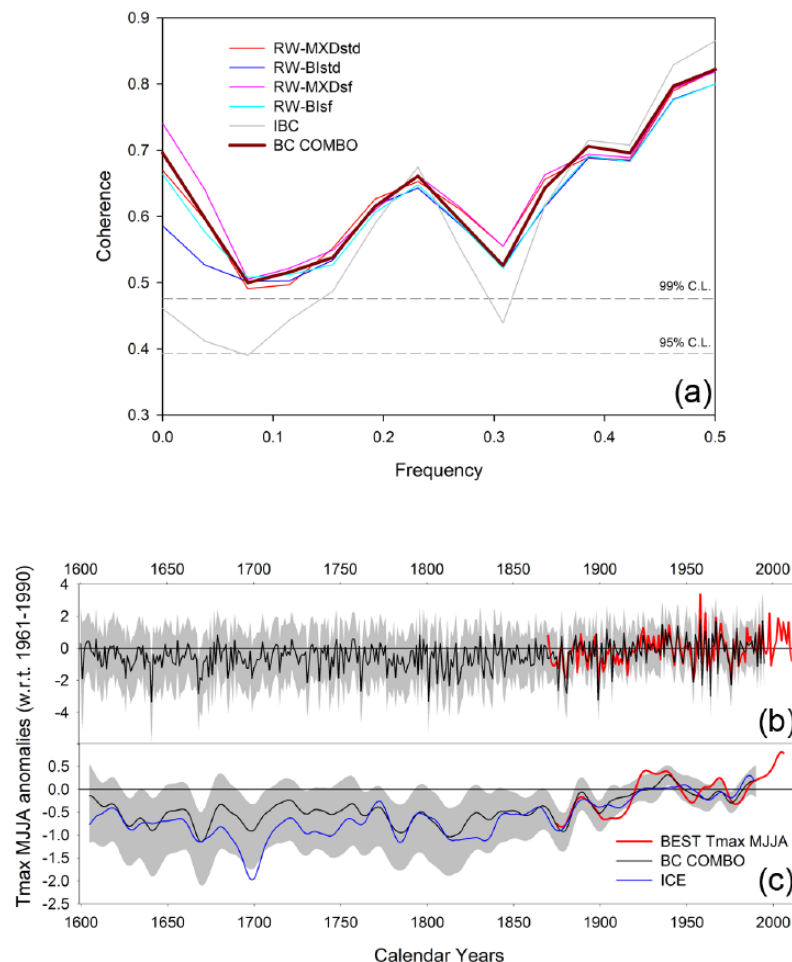


Figure 7. (a) Coherency spectral analysis between the five BC reconstruction variants and the BEST MJJA Tmax temperature series over the 1870–1995 period. (b) Weighted BC COMBO reconstruction and BEST MJJA Tmax data. (c) 20-year spline smoothed BC COMBO reconstruction compared to Icefields reconstruction and BEST data. For (b + c), the weighted BC COMBO time-series has not been re-scaled to the instrumental data allowing the RMSE from each chronology reconstruction variant to be used to derive a full-range 2-sigma error. Note that these error ranges do not incorporate the extra uncertainty indicated by the weaker expressed signal strength prior to 1650 (Figure 3). RW: ring-width; MXD: maximum latewood density; BI: Blue Intensity; IBC: Interior British Columbia; ICE: Icefields; BC: British Columbia; BEST: Berkeley Earth Surface Temperature; RMSE: root mean square error.

comparison to earlier instrumental data (Table 5) provided only minimal help in ascertaining which of the reconstructions best represented past MJJA maximum temperatures. We therefore concluded that all variants expressed a possible probabilistic scenario of past summer temperature for the region and utilised the RMSE error over the 1870–1900 period to weight the different series together to derive the weighted BC COMBO series (with an associated full 2-sigma error range derived from the different reconstruction variants). The BC COMBO series agrees well with the independent ICE reconstruction from the neighbouring Rocky Mountains to the east (Luckman and Wilson, 2005) – both series indicating a $\sim 1^{\circ}\text{C}$ warming of summer maximum temperatures from the ‘LIA’ to 20th century. Whether using RW, MXD or BI, the optimal response to maximum summer temperatures, as originally proposed by Wilson and Luckman (2003), still holds even

when SF detrending (Melvin and Briffa, 2008) is utilised. Further testing of this Tmax optimal response hypothesis is, however, needed through other regional studies.

Taking into account, uncertainties related to different detrending methodologies and the shortness of the instrumental data, it is not possible from this study to quantify which parameter is best for reconstructing past summer temperatures in this region. Rather, our results indicate that MXD and BI, as they are both measures of lignin content in the latewood, can be used as proxies of past summer temperatures. At this time, we still recommend, if funds allow, that MXD is the parameter of choice as there are still many potential uncertainties with the use of BI data. Despite Björklund et al. (2014) and Rydval et al. (2014) proposing solutions to overcome biases related to the heartwood/sapwood colour transition and discolouration of sub-fossil samples in Scots pine, these issues still

need to be explored in other regions and for other conifer species. Also, the relatively tight range in between-sample (and site) variance seen for BI compared to MXD (Table 1) could suggest potential for a systematic limitation for this parameter to capture centennial and longer scale variability. However, SF detrending (Melvin and Briffa, 2008) did significantly improve the BI parameter's ability to capture secular scale variation compared to traditional detrending methods (Figure 6a). However, we would also caution that SF detrending is still an experimental method which also requires further experimentation.

The cheapness of measuring BI using the CooRecorder suite (Larsson, 2013) will allow many more tree-ring laboratories to experiment with this parameter. It is too early to say whether BI could replace MXD. Much more experimentation is needed, not only on different conifer species but also using long well replicated data-sets of living and sub-fossil material. Some results in this paper suggest that BI measurements may struggle to capture centennial variability, but this can only be tested if BI is measured from samples where MXD (or RW) portray distinct low frequency variability. Therefore, further work will aim to measure BI on the ICE samples where lower frequency information can be gleaned from the MXD data (Luckman and Wilson, 2005). However, western Canada is not an ideal location to truly test BI because of the relative shortness of the instrumental record. Therefore, we propose that a true robust assessment can only be made by focusing on the millennial length living/historical/sub-fossil composite chronologies from Europe where long instrumental series exist (Büntgen et al., 2006; Esper et al., 2012; Grudd, 2008; Gunnarson et al., 2011; Wilson et al., 2011).

Acknowledgements

Original MXD measurements were made at the Lamont Doherty Earth Observatory Tree-Ring Laboratory by Rob Wilson. We are indebted to Ed Cook and Paul Krusic for providing software to undertake the Signal-Free detrending. Many thanks to Bjorn Gunnarson, Rosanne D'Arrigo, Jan Esper, Jesper Björklund, Meritxell Ramirez Olle and Mike Jarvis for their comments and discussion on this work and to the reviewers for highlighting where clarification was needed.

Funding

This work was part funded through Blue Intensity development aspects of the UK Leverhulme Trust and Natural Environment Research Council (NERC) projects, 'RELIC: Reconstructing 8000 years of Environmental and Landscape change in the Cairngorms (F/00 268/BG)' and 'SCOT2K: Reconstructing 2000 years of Scottish climate from tree-rings (NE/K003097/1)'. Miloš Rydval's PhD is funded by the Carnegie Trust for the Universities of Scotland. Initial sample collection was funded by an NSERC Discovery Grant to Brian Luckman with the field assistance of Don Youngblut.

References

- Anchukaitis KJ, Breitenmoser P, Briffa KR et al. (2012) Tree rings and volcanic cooling. *Nature Geoscience* 5: 836–837.
- Anchukaitis KJ, D'Arrigo RD, Andreu-Hayles L et al. (2013) Tree-ring reconstructed summer temperatures from north-western North America during the last nine centuries. *Journal of Climate* 26(10): 3001–3012.
- Babst F, Frank D, Büntgen U et al. (2009) Effect of sample preparation and scanning resolution on the Blue Reflectance of *Picea abies*. *TRACE* 7: 188–195.
- Biondi F, Perkins DL, Cayan DR et al. (1999) July temperature during the second millennium reconstructed from Idaho tree rings. *Geophysical Research Letters* 26: 1445–1448.
- Björklund JA, Gunnarson BE, Seftigen K et al. (2014) Is blue intensity ready to replace maximum latewood density as a strong temperature proxy? A tree-ring case study on Scots pine from northern Sweden. *Climate of the Past Discussions* 9: 5227–5261.
- Briffa KR and Jones PD (1990) Basic chronology statistics and assessment. In: Cook ER and Kairiukstis LA (eds) *Methods of Dendrochronology: Applications in the Environmental Sciences*. Dordrecht: Kluwer Academic Publishers, pp. 137–152.
- Briffa KR and Melvin TM (2010) A closer look at regional curve standardization of tree-ring records: Justification of the need, a warning of some pitfalls, and suggested improvements in its application. In: Hughes MK, Diaz HF and Swetnam TW (eds) *Dendroclimatology: Progress and Prospects*. Dordrecht: Springer Verlag.
- Briffa KR, Osborn TJ, Schweingruber FH et al. (2001) Low-frequency temperature variations from a northern tree ring density network. *Journal of Geophysical Research* 106(D3): 2929–2941.
- Büntgen U, Frank DC, Grudd H et al. (2008) Long-term summer temperature variations in the Pyrenees. *Climate Dynamics* 31: 615–631.
- Büntgen U, Frank DC, Nievergelt D et al. (2006) Summer temperature variations in the European Alps, AD 755–2004. *Journal of Climate* 19: 5606–5623.
- Campbell R, McCarroll D, Loader NJ et al. (2007) Blue intensity in *Pinus sylvestris* tree-rings: Developing a new palaeoclimate proxy. *The Holocene* 17: 821–828.
- Campbell R, McCarroll D, Robertson I et al. (2011) Blue intensity in *Pinus sylvestris* tree rings: A manual for a new palaeoclimate proxy. *Tree-Ring Research* 67: 127–134.
- Cook ER and Peters K (1981) The smoothing spline: A new approach to standardizing forest interior tree-ring width series for dendroclimatic studies. *Tree-Ring Bulletin* 41: 45–53.
- Cook ER, Briffa KR and Jones PD (1994) Spatial regression methods in dendroclimatology: A review and comparison of two techniques. *International Journal of Climatology* 14: 379–402.
- Cook ER, Krusic PJ, Anchukaitis KJ et al. (2013) Tree-ring reconstructed summer temperature anomalies for temperate East Asia since 800 C.E. *Climate Dynamics* 41: 2957–2972.
- D'Arrigo R, Wilson R and Anchukaitis K (2013) Volcanic cooling signal in tree-ring temperature records for the past millennium. *Journal of Geophysical Research: Atmospheres* 118(16): 9000–9010.
- D'Arrigo R, Wilson R and Jacoby G (2006) On the long-term context for late 20th century warming. *Journal of Geophysical Research* 111: D03103. DOI: 10.1029/2005JD006352.
- D'Arrigo R, Jacoby G, Frank D et al. (2001) 1738 years of Mongolian temperature variability inferred from a tree-ring record of Siberian pine. *Geophysical Research Letters* 28: 543–546.
- D'Arrigo R, Wilson R, Liepert B et al. (2008) On the 'Divergence Problem' in Northern Forests: A review of the tree-ring evidence and possible causes. *Global and Planetary Change* 60: 289–305.
- Esper J, Büntgen U, Luterbacher J et al. (2013a) Testing the hypothesis of post-volcanic missing rings in temperature sensitive dendrochronological data. *Dendrochronologia* 31(3): 216–222.
- Esper J, Frank DC, Büntgen U et al. (2010) Trends and uncertainties in Siberian indicators of 20th century warming. *Global Change Biology* 16: 386–398.
- Esper J, Frank DC, Timonen M et al. (2012) Orbital forcing of tree-ring data. *Nature Climate Change* 2: 862–866.
- Esper J, Frank DC, Wilson RJS et al. (2005) Effect of scaling and regression on reconstructed temperature amplitude for the past millennium. *Geophysical Research Letters* 32: L07711. DOI: 10.1029/2004GL021236.

- Esper J, Schneider L, Krusic PJ et al. (2013b) European summer temperature response to annually dated volcanic eruptions over the past nine centuries. *Bulletin of Volcanology* 75: 736.
- Esper J, Shiyatov SG, Mazepa VS et al. (2003) Temperature-sensitive Tien Shan tree-ring chronologies show multi-centennial growth trends. *Climate Dynamics* 8: 699–706.
- Frank D, Esper J and Cook ER (2007) Adjustment for proxy number and coherence in a large-scale temperature reconstruction. *Geophysical Research Letters* 34. DOI: 10.1029/2007GL030571.
- Gindl W, Grabner M and Wimmer R (2000) The influence of temperature on latewood lignin content in treeline Norway spruce compared with maximum density and ring width. *Trees: Structure and Function* 14: 409–414.
- Grudd H (2008) Torneträsk tree-ring width and density AD 500–2004: A test of climatic sensitivity and a new 1500-year reconstruction of north Fennoscandian summers. *Climate Dynamics* 31: 843–857.
- Gunnarson BE, Linderholm HW and Moberg A (2011) Improving a tree-ring reconstruction from west-central Scandinavia: 900 years of warm-season temperatures. *Climate Dynamics* 36: 97–108.
- Harris I, Jones PD, Osborn TJ et al. (2014) Updated high-resolution grids of monthly climatic observations – The CRU TS3.10 dataset. *International Journal of Climatology* 34: 623–642.
- Hughes MK, Schweingruber FH, Cartwright D et al. (1984) July–August temperature at Edinburgh between 1721 and 1975 from tree-ring density and width data. *Nature* 308: 341–343.
- Hughes MK, Vaganov E, Shiyatov S et al. (1999) Twentieth-century summer warmth in northern Yakutia in a 600 year context. *The Holocene* 9: 603–608.
- Jones PD, Briffa KR, Osborn TJ et al. (2009) High-resolution palaeoclimatology of the last millennium: A review of current status and future prospects. *The Holocene* 19(1): 3–49.
- Larsson L (2013) CooRecorder program of the CooRecorder/Cdendro package version 7.6. Available at: <http://www.cybis.se/forfun/dendro/>.
- Luckman BH and Wilson RJS (2005) Summer temperature in the Canadian Rockies during the last millennium: A revised record. *Climate Dynamics* 24: 131–144.
- McCarroll D, Pettigrew E, Luckman A et al. (2002) Blue reflectance provides a surrogate for latewood density of high-latitude pine tree rings. *Arctic, Antarctic, and Alpine Research* 34: 450–453.
- Mann ME, Fuentes JD and Rutherford S (2012) Underestimation of volcanic cooling in tree-ring based reconstructions of hemispheric temperatures. *Nature Geoscience* 5: 202–205.
- Melvin TM and Briffa KR (2008) A ‘Signal-Free’ approach to dendroclimatic standardisation. *Dendrochronologia* 26: 71–86.
- Osborn TJ, Briffa KB and Jones PD (1997) Adjusting variance for sample size in tree-ring chronologies and other regional mean timeseries. *Dendrochronologia* 15: 89–99.
- Peterson TC, Easterling DR, Karl TR et al. (1998) Homogeneity adjustments of in situ atmospheric climate data: A review. *International Journal of Climatology* 18(13): 1493–1517.
- Rohde R, Muller RA, Jacobsen R et al. (2013) A new estimate of the average earth surface land temperature spanning 1753 to 2011. *Geoinformatics & Geostatistics: An Overview* 1: 1. doi: 10.4172/2327-4581.1000101.
- Rydval M, Larsson LA, McGlynn L et al. (2014) Blue Intensity for dendroclimatology: Should we have the blues? Experiments from Scotland. *Dendrochronologia* 32: 191–204.
- Salzer M and Kipfmüller K (2005) Reconstructed temperature and precipitation on a millennial timescale from tree-rings in the southern Colorado plateau, U.S.A. *Climatic Change* 70: 465–487.
- Schweingruber FH and Briffa KR (1996) Tree-ring density networks for climate reconstruction. In: Jones PD, Bradley RS and Jouzel J (eds) *Climatic Variations and Forcing Mechanisms of the Last 2000 Years*. Berlin and Heidelberg: Springer Verlag, pp. 43–66.
- Schweingruber FH, Fritts HC, Braker OU et al. (1978) The X-ray technique as applied to dendroclimatology. *Tree-Ring Bulletin* 38: 61–91.
- Sheppard PR and Wiedenhoef A (2007) An advancement in removing extraneous color from wood for low-magnification reflected-light image analysis of conifer tree rings. *Wood and Fiber Science* 39: 173–183.
- Sheppard PR, Graumlich LJ and Conkey LE (1996) Reflected-light image analysis of conifer tree rings for reconstructing climate. *The Holocene* 6: 62–68.
- Wigley TML, Briffa KR and Jones PD (1984) On the average of correlated time series, with applications in dendroclimatology and hydrometeorology. *Journal of Climate and Applied Meteorology* 23: 201–213.
- Wilson RJS and Elling W (2004) Temporal instabilities of tree-growth/climate response in the Lower Bavarian Forest Region: Implications for dendroclimatic reconstruction. *Trees: Structure and Function* 18(1): 19–28.
- Wilson RJS and Luckman BH (2003) Dendroclimatic reconstruction of maximum summer temperatures from upper tree-line sites in Interior British Columbia. *The Holocene* 13(6): 853–863.
- Wilson RJS, D’Arrigo R, Buckley B et al. (2007a) A matter of divergence – Tracking recent warming at hemispheric scales using tree-ring data. *Journal of Geophysical Research: Atmospheres* 112: D17103. DOI: 10.1029/2006JD008318.
- Wilson RJS, Loader N, Rydval M et al. (2011) Reconstructing Holocene climate from tree rings – The potential for a long chronology from the Scottish Highlands. *The Holocene* 22(1): 3–11.
- Wilson RJS, Wiles G, D’Arrigo R et al. (2007b) Cycles and shifts: 1300-years of multi-decadal temperature variability in the Gulf of Alaska. *Climate Dynamics* 28: 425–440.
- Yanosky TM and Robinove CJ (1986) Digital image measurement of the area and anatomical structure of tree rings. *Canadian Journal of Botany* 64: 2896–2902.
- Youngblut DK and Luckman BH (2008) Maximum June–July temperatures in the southwest Yukon Region over the last three hundred years reconstructed from tree-rings. *Dendrochronologia* 25: 153–166.